

# Structure, stability, and electronic properties of the *i*-AlPdMn quasicrystalline surface

M. Krajčí<sup>1,2</sup> and J. Hafner<sup>1</sup>

<sup>1</sup>*Institut für Materialphysik and Center for Computational Materials Science, Universität Wien, Sensengasse 8/12, A-1090 Wien, Austria*

<sup>2</sup>*Institute of Physics, Slovak Academy of Sciences, Dúbravská cesta 9, SK-84511 Bratislava, Slovak Republic*

(Received 6 October 2004; published 18 February 2005)

The structure, stability, and electronic properties of a fivefold surface of an icosahedral (*i*) Al-Pd-Mn alloy have been investigated using *ab initio* density-functional methods. Structural models for a series of rational approximants to the quasicrystalline structure of bulk *i*-AlPdMn have been constructed using the cut-and-projection technique with triacontahedral acceptance domains in the six-dimensional hyperspace according to the Katz-Gratias-Boudard model. This leads to a real-space structure describable in terms of interpenetrating Mackay and Bergman clusters. A fivefold surface has been prepared by cleaving the bulk structure along a plane perpendicular to a fivefold axis. The position of the cleavage plane has been chosen such as to produce a surface layer with a high atomic density. The atomic structure of these surfaces can be described by a P1 tiling by pentagons, thin rhombi, pentagonal stars, and a “boat”—in terms of a cut-and-projection model the decagonal acceptance domain of the P1 tiling corresponds to the maximal cross section of the triacontahedra defining the three-dimensional quasicrystal. The vertices of the P1 tiling are occupied by Pd atoms surrounded by pentagonal motifs of Al atoms. For the *ab initio* calculations we have prepared slab models of the surface based on the 3/2 and 2/1 approximants and containing up to 357 atoms in the computational cell. The analysis of the surface charge density shows flat minima at the vertices of the P1 tiling and strong charge depletion in some of the pentagonal tiles (“surface vacancies”). Both observations are in agreement with scanning tunneling microscopy studies of these surfaces. Structural relaxations have been performed only for the 2/1 models with up to 205 atoms/cell. The calculations demonstrate that the skeleton of the P1 tiling fixed by the transition-metal atoms represents a stable surface termination, but considerable rearrangement of the Al atoms and large relaxations of the interlayer distances. The analysis of the surface electronic structure shows that the deep structure-induced pseudogap just above the Fermi level is filled up at the surface as a consequence of the structural disorder in the arrangement of the Al atoms at the surface and of a shift of both the Pd and Mn *d* band to lower binding energy. The *d* band shift at the surface is in good agreement with observations based on photoelectron and Auger spectroscopies.

DOI: 10.1103/PhysRevB.71.054202

PACS number(s): 61.44.Br, 68.35.Bs, 71.20.-b, 71.23.Ft

## I. INTRODUCTION

During the last decade great attention has been focused on the properties of quasicrystalline surfaces. Quasicrystalline surfaces and coatings exhibit high hardness, good tribological properties such as low surface friction and high oxidation resistance, i.e., properties important for many technological applications. The structure of *i*-AlPdMn and its surface properties have been intensively studied by various experimental methods. A low-energy electron diffraction (LEED) analysis<sup>1,2</sup> showed that the fivefold surface of *i*-AlPdMn conserves the bulk quasicrystalline structure. Scanning tunneling microscope (STM) investigations of icosahedral AlPdMn (Refs. 3 and 4) revealed a set of atomically flat terraces with steps of several different heights in a succession forming a Fibonacci-like sequence. The STM images of the *i*-AlPdMn surface show quasicrystalline order at the surface and atomic scale features with local fivefold symmetry. Schaub *et al.*<sup>4</sup> and Barbier *et al.*<sup>3</sup> produced high-resolution STM images of terraces revealing a dense distribution of dark pentagonal holes. The interpretation of the experimental results was based on a bulk termination of the ideal quasicrystalline structure. Papadopolos *et al.*<sup>5</sup> mapped high-resolution STM images of a fivefold surface of *i*-AlPdMn to a planar tiling derived from a geometrical model of icosahedral AlPdMn.

The experimentally derived tiling of the surface matches a geometrical tiling derived from the structural model. It was found that the atomic positions on the terraces correspond exactly to cuts across the basic atomic clusters of the bulk structure, the so-called Bergman and pseudo-Mackay clusters. The dark pentagonal holes in the STM pictures correspond to the Bergman clusters in the bulk layers. Zheng *et al.*<sup>6</sup> investigated the structure of the fivefold surface of the *i*-AlPdMn using x-ray photoelectron diffraction (XPD). They analyzed the structural relaxation at the quasicrystal surface and found differences in the interlayer spacing of surface layers in comparison to the spacing of atomic layers in the bulk. Similar findings were reported also by the LEED analysis.<sup>1,2</sup> The electronic structure of quasicrystalline surfaces was studied using photoelectron and Auger electron spectroscopies.<sup>7</sup> It was found that in *i*-AlPdMn the pseudogap characteristic for the electronic density of states (DOS) of the bulk is not leveled out at the surface, but it can be restored by annealing at sufficiently high temperatures. The reader can find a summary of the progress in determining structure and properties of quasicrystalline surfaces in Refs. 8 and 2.

Scanning tunneling microscopy is one of the most frequently used experimental probes for the analysis of the local structure of quasicrystalline surfaces. However, as STM im-

ages reproduce actually only the electronic charge density at the surface and not its atomic structure, independent complementary information from theoretical models linking the atomic positions and the electron density is thus very desirable. In this paper we report our results of a structural modeling of the *i*-AlPdMn surface, the charge density distribution at the surface, of investigations of surface relaxation and reconstruction, and calculations of the surface electronic properties. Our paper is organized as follows. In Sec. II the reference model for the structure of bulk *i*-AlPdMn and the choice of the cleavage plane resulting in a surface with fivefold symmetry are described. *Ab initio* investigations of surfaces are routinely carried out on slab models with a separating vacuum layer and periodic boundary conditions. The thickness of the slab perpendicular to the surface should be sufficiently large to represent the bulk structure terminated by the surface. We shall consider two structural models of different thicknesses. Their construction is described in Sec. II C. The surface relaxation, the influence of the bulk termination on the atomic positions, and charge distributions are reported in Sec. V. The electronic density of states in bulk and at the surface are compared in Sec. VI. We summarize in Sec. VII. Our results demonstrate that the skeleton of the fivefold periodic surface structure as resulting from the cleavage of the bulk-structure along a close-packed plane is conserved: The vertices of the tiling of the surface are occupied by transition-metal atoms, they remain at their positions upon relaxation. The decoration of the tiles, however, is distorted quite appreciably. The surface-induced atomic displacements also result in a leveling of the structural pseudogap in the electronic DOS close to the Fermi level.

## II. STRUCTURAL MODEL OF SURFACE OF *i*-AlPdMn

### A. Structural model of *i*-AlPdMn

A structural model of a quasicrystalline surface of *i*-AlPdMn is obtained from a model of the icosahedral AlPdMn quasicrystal by cleaving it at a proper plane. The icosahedral AlPdMn phase belongs to the icosahedral F-type (face centered) quasicrystals. A structural model of this class of quasicrystals was first proposed by Cornier *et al.*<sup>9</sup> on the basis of diffraction data for *i*-AlCuFe. In the literature this model is mostly referred to as the model of Katz and Gratias<sup>10</sup> (KG model). The model consists of three types of atomic surfaces decorating the vertices of a six-dimensional (6D) hypercubic lattice. Boudard *et al.*<sup>11</sup> and de Boissieu *et al.*<sup>12</sup> successfully applied the model to the description of the structure of icosahedral AlPdMn. They proposed a shell structure of the atomic surfaces defining the chemical ordering of the aluminum and transition metal atoms in the quasicrystal. As we consider the correct chemical ordering to be of great importance, we denote this model of *i*-AlPdMn as the model of Katz-Gratias-Boudard (KGB model).

Recently Gratias *et al.*<sup>13</sup> presented a detailed study of the atomic clusters encountered in F-type quasicrystals. Significant contributions to the understanding of the real-space atomic structure of the *i*-AlPdMn were made by Elser,<sup>14</sup> Papadopolos *et al.*,<sup>15</sup> and Kramer *et al.*<sup>16</sup> Elser recognized that

the KG model of *i*-AlPdMn can be interpreted as a three-dimensional Penrose tiling with the vertices decorated by Bergman and pseudo-Mackay clusters. On the basis of Elser's ideas Papadopolos, Kramer, and co-workers proposed a tiling model of *i*-AlPdMn. The authors have labeled the model as the  $\mathcal{M}$  model. They decorated the 3D Penrose tiling in accordance with the F character of the 6D lattice. In its 6D representation the  $\mathcal{M}$  model has also three atomic surfaces like the KG model, but their shapes are somewhat more complex. A purely 6D model of *i*-AlPdMn was proposed also by Yamamoto.<sup>17,18</sup> His model consists of three rather complex multiply connected atomic surfaces at the same nodes of the 6D lattice as in the KG and  $\mathcal{M}$  models, but in addition there is also an atomic surface at the midedge positions of the hypercubic lattice. Unfortunately, in this sophisticated model the chemical ordering is not well-defined. Most of the atomic surfaces in the model of Yamamoto have mixed Al/TM occupations. A computer-simulation of the structure of *i*-AlPdMn, based on *ab initio* density functional calculations of the total energies and interatomic forces was presented by Quandt and Elser.<sup>19</sup> However, their model consists of 65 atoms only and is not large enough to be representative for any surface modeling.

It was demonstrated that the surface of *i*-AlPdMn is consistent with a bulk termination of the KGB model.<sup>20</sup> The KGB model agrees well with the diffraction data, density, and stoichiometry.<sup>9,11,21,22</sup> The stoichiometry of the KGB model,  $\text{Al}_{0.7073}\text{Pd}_{0.2063}\text{Mn}_{0.0864}$ , is in very good agreement with the experimentally determined composition of  $\text{Al}_{0.711}\text{Pd}_{0.202}\text{Mn}_{0.087}$  (Ref. 3) or  $\text{Al}_{0.705}\text{Pd}_{0.21}\text{Mn}_{0.085}$  (Ref. 23). The KGB model also provides very good agreement of the calculated photoemission spectra with the experimental ones.<sup>24</sup> For the purpose of electronic structure calculations this model is the most suitable. The reason is not only its satisfactory description of the chemical ordering, but the simplicity of this model in 6D space which allows us to impose a linear phason strain and thus to construct well-defined finite approximants.

The KGB model of *i*-AlPdMn starts from a six-dimensional (6D) cubic lattice.<sup>25</sup> The lattice nodes are decorated by three kinds of triacontahedral atomic surfaces: a triacontahedron at the "even" nodes ( $n_0=[000000]$ ) and the "odd" nodes ( $n_1=[100000]$ ) and a smaller triacontahedron at the body-centered  $bc_1$  positions ( $bc_1=\frac{1}{2}[111111]$ ). The  $bc_0$  positions ( $bc_0=\frac{1}{2}[011111]$ ) are empty. The atomic surface at the  $n_0$  node is truncated by its intersections with its 12 images displaced by  $\tau^3$  [with the golden mean  $\tau=(1+\sqrt{5})/2$ ] along the fivefold axes. The fivefold radii of the large triacontahedra at  $n_0$  and  $n_1$  are  $\tau$  and the radius of the smaller one at  $bc_1$  is  $\tau^{-1}$ . The inequivalence of the atomic surfaces centered at the even and odd nodes and at the  $bc_0$  and  $bc_1$  nodes breaks the simple cubic symmetry of the 6D lattice and leads to a face-centered superstructure. The atomic surfaces have an inner shell structure determining the chemical order of the quasicrystal which has a significant influence on the electronic properties of the structural model. The large triacontahedra at the even nodes  $n_0$  and the odd nodes  $n_1$  contain small triacontahedra in the center occupied by Mn atoms. At the  $n_1$  node the Mn core is surrounded by an outer

TABLE I. Structural data of approximants to *i*-AlPdMn and of the slab models for the fivefold surface. Cell dimensions  $d_i$ ,  $i=x,y,z$  in Å, number of atoms  $N_a$ , and chemical composition.

Model	$d_x$	$d_y$	$d_z$	$N_a$	$N(\text{Al})$	$N(\text{Pd})$	$N(\text{Mn})$
2/1 bulk	20.31	20.31	20.31	544	372	124	48
2/1 MS	23.88	20.31	6.60	205	137	54	14
2/1 M	23.88	20.31	4.08	136	96	36	4
3/2 bulk	32.86	32.86	32.86	2292	1612	472	208
3/2 MS	39.40	32.86	6.60	535	364	132	39
3/2 M	39.40	32.86	4.08	357	251	92	14
5/3 bulk	53.17	53.17	53.17	9700	6844	2012	844
5/3 MS	62.51	53.17	6.60	1401	965	340	96
5/3 M	62.51	53.17	4.08	930	663	236	31

Al shell. At the even node  $n_0$  the Mn core is surrounded by an inner Pd shell and an outer Al shell. In our version of the KGB model the radii of the inner shells containing transition metal atoms are  $2\tau^{-1}$ ,  $2\tau^{-2}$  at  $n_0$ , and  $\tau^{-1}$  at  $n_1$ . The body-centered  $bc_1$  positions are decorated with Pd atoms.

For any numerical calculation one needs well-defined finite models. In the case of quasicrystals a systematic approach to the construction of such models is available, based on the concept of quasicrystalline approximants. Periodic quasicrystalline approximants are constructed by imposing a linear phason strain, i.e., a certain deformation of the atomic surfaces in the 6D hypercubic lattice. This procedure is equivalent to a replacement of the golden mean  $\tau$  in the corresponding formalism by a rational approximant given in terms of the Fibonacci numbers  $F_n$ ,  $\tau_n = F_{n+1}/F_n$  with  $F_{n+1} = F_n + F_{n-1}$  and  $F_0 = 0$ ,  $F_1 = 1$ ,  $n = 0, 1, 2, \dots$ . The effect of this procedure is the replacement of irrational vectors, e.g.,  $\langle \tau, 1, 0 \rangle$ , in perpendicular space by rational ones,  $\langle F_{n+1}, F_n, 0 \rangle$ . We note that this replacement is performed only in perpendicular space; in parallel (physical) space the vectors remain irrational. In the physical space the approximants thus have exact fivefold local axes. The unit cells of all approximants have cubic shape, the edge  $d_n$  of the unit cell of the  $n$ th approximant is  $d_n = [2/\sqrt{(\tau+2)}]\tau^{n+1}a_{qc}$ , where  $a_{qc}$  is the quasilattice constant equal to 4.56 Å. The 1/1 approximant to *i*-AlPdMn has 128 atoms/cell, the 2/1, 3/2, and 5/3 approximants have 544, 2292, and 9700 atoms/cell, respectively, see Table I. The space-group symmetry is  $P2_13$  for all approximants.

### B. Atomic clusters in *i*-AlPdMn

The real-space structure of quasicrystals is frequently discussed in terms of atomic clusters possessing icosahedral symmetry. Their identity and stability, however, is a subject of controversial discussions. The F-type icosahedral phases are often designated as the ‘‘Mackay-type’’ structures as opposed to the ‘‘Bergman-type’’ structures like AlCuLi or the ‘‘Tsai-type’’ such as CdYb. However, it was already pointed out several times<sup>10,14,15</sup> that F-type icosahedral structures contain both Mackay- and Bergman-type clusters. They are not independent structural units, as the clusters are mutually interpenetrating. We note that the ‘‘Mackay’’ and ‘‘Bergman’’

clusters in *i*-AlPdMn are a little different from those encountered in various complex intermetallic crystalline structures. Instead of using the term pseudo-Mackay or pseudo-Bergman we shall, in agreement with Gratias *et al.*,<sup>13</sup> call the clusters the *M* and *B* clusters. Each bc-site of the real-space structure of *i*-AlPdMn is a center of a *B* cluster. The *B* cluster consists of 33 atoms with a Pd atom in the center. The *M* clusters are centered by Mn atoms. The first atomic shell of the *M* cluster is very irregular. Seven or eight atoms occupy vertices of a small dodecahedron, but their spatial arrangement around the central Mn atom is irregular with respect to the icosahedral symmetry. The clusters and their distribution in the F-type quasicrystals have been analyzed in the work of Gratias *et al.*<sup>13</sup> It was stressed that the *B* clusters are extremely robust. Any model based on two main atomic surfaces at the even and odd nodes and a small surface at bc generates *B* clusters as a natural consequence of the geometry of 6D lattice. Gratias *et al.* suggested using the *B* clusters as guidelines for discussing the atomic structure and physical properties of the F-type quasicrystals. They consider the *B* clusters as the best candidates for identifying the mean structural features of these quasicrystals. In particular, the positions of terraces observed in STM images of *i*-AlPdMn surfaces are matched to layers characterized by a density of the *B* clusters and their distribution pattern.

### C. Structural model of a fivefold surface

A structural model of a quasicrystalline surface is obtained from the model of an icosahedral approximant by cleaving at a proper plane perpendicular to one of the fivefold axes. The position of the plane bounding the quasicrystal should correspond to a plane of high atomic density.<sup>26</sup> The average atomic density of a fivefold surface has been determined<sup>1</sup> as 0.136 atoms per Å<sup>2</sup>. Figure 1 shows a projection of the position of atoms in the 5/3-approximant onto the  $(x,y)$  plane. The orientation of one of the fivefold axes lying in this plane is indicated by the arrow. The slope of the projected fivefold planes with respect to the  $x$  axis is  $\beta = 58.282^\circ$ ,  $\sin(\beta) = \tau/\sqrt{(\tau+2)}$ . The projection displays the atomic density in the fivefold planes perpendicular to the  $(x,y)$  plane. One can observe that planes with high atomic density are separated by (pseudo)gaps of low atomic density.

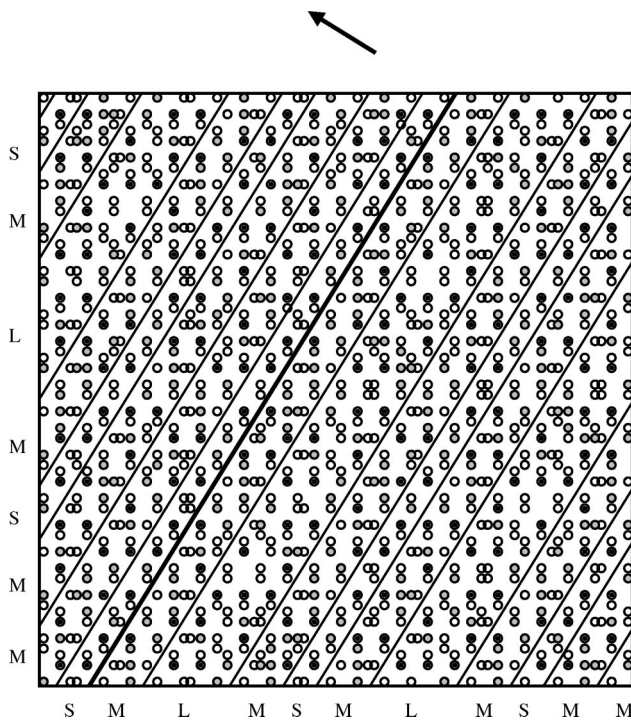


FIG. 1. Projection of the atomic positions of the 5/3-approximant to icosahedral AlPdMn onto the  $(x,y)$  plane. The circles represent the projected positions of atoms: Al: open circles, Pd: shaded circles, and Mn: small closed circles. The arrow shows the direction of one of the pentagonal axes parallel to the plane. The figure demonstrates the existence of dense atomic layers separated by density gaps (“empty streets”). They can be seen by viewing the figure from a low angle. The position of the density gaps are marked by straight lines. The structural model can be decomposed into a sequence of slabs of three different thicknesses, cf. text. The slabs are marked by S, M, and L and form a Fibonacci-like sequence. A model of the surface is obtained by cleaving the structure along a plane, located in the density gap, marked by the thick straight line.

These “empty streets” can be easily seen by viewing the figure from a low angle. We note that these density-pseudogaps have a meaning only in a geometrical sense, if atoms are considered as points. They are well-resolved only because the other atomic layers have a denser spacing. The characteristic spacing between atomic layers on both sides of the pseudogap is  $1.56 \text{ \AA}$ , while the interlayer distance between the next two layers is only  $0.48 \text{ \AA}$ . A layer spacing of  $1.56 \text{ \AA}$  is not extraordinarily large. For comparison, the interlayer spacing of  $\langle 111 \rangle$  atomic planes in fcc Al is  $2.34 \text{ \AA}$ . Nevertheless, the pseudogaps in the atomic density between high-density planes are natural cleavage planes of the quasicrystal.<sup>26</sup> The distances between the atomic density minima form a Fibonacci sequence. One can recognize three different distances:  $s=2.52 \text{ \AA}$ ,  $m=4.08 \text{ \AA}$ , and  $l=s+m=6.60 \text{ \AA}$ . The theoretical values of these distances were derived and reported by Papadopolos *et al.*<sup>5</sup> The sequence of the distances  $s, m, l$  corresponds to the sequence of terraces in the STM images measured by Schaub *et al.*<sup>4</sup> While Schaub *et al.* observe only a Fibonacci sequence of terraces with heights  $m$  and  $l$ , Shen *et al.*<sup>27</sup> found also a lower terrace height comparable with  $s$ .

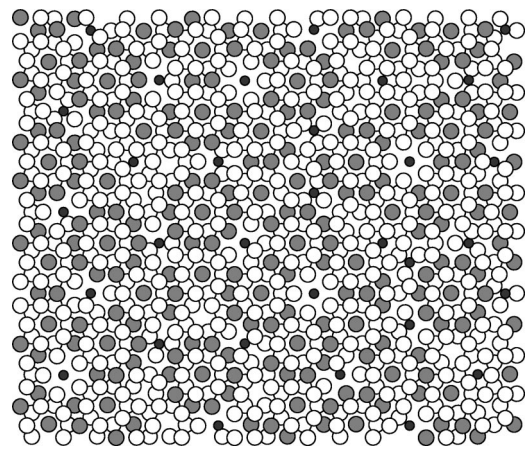


FIG. 2. The atomic structure of the M slab (R surface). Same symbols as in Fig. 1. The structure can be interpreted in terms of interpenetrating Bergman ( $B$ ) and (pseudo)Mackay ( $M$ ) clusters. The regular decagonal rings of Pd atoms correspond to the  $B$  clusters. Each  $B$  cluster is centered by a Pd atom. In addition a regular arrangement of atoms with pentagonal symmetry is observed also around most Mn atoms. These are centers of the  $M$  clusters. The  $B$  and  $M$  clusters are mutually interpenetrating. An outer part of the  $B$  cluster is shared with  $M$  and vice versa. This competition of the clusters often leads to an incompleteness of one of them.

A quasicrystalline approximant can be thus decomposed into a sequence of slabs of three different thicknesses. According to their thickness  $s, m$ , and  $l$  we denote these slabs as S, M, and L, respectively. The S slab consists of three layers of atoms, the M slab consists of five, and the L slab of eight layers of atoms. A model of a quasicrystalline surface is created by cleaving the approximant at a plane separating the slabs. As a model of a surface of the AlPdMn quasicrystal we have chosen the surface of the M slab. This choice corresponds to one of the most frequently reported terminations of  $i$ -AlPdMn perpendicular to a fivefold axis. In the notation of Papadopolos *et al.*<sup>5</sup> it is equivalent to the R termination.

Figure 2 shows the atomic structure of the pentagonal surface. The structure of  $i$ -AlPdMn can be interpreted in terms of interpenetrating Bergman ( $B$ ) and (pseudo)Mackay ( $M$ ) clusters.<sup>13</sup> In the figure one can easily recognize a regular structure of decagonal rings of Pd atoms. These rings correspond to the  $B$  clusters. Each  $B$  cluster is centered by a Pd atom. In addition a regular arrangement of atoms with pentagonal symmetry is observed also around most of the Mn atoms. These are centers of the  $M$  clusters. The  $B$  and  $M$  clusters are mutually interpenetrating. An outer part of a  $B$  cluster is shared with a  $M$  cluster and vice versa. This overlap of the clusters leads to a conflict between their building principles and chemical decorations, eventually causing a substitutional defect or incompleteness of one of the clusters. We note that the atomic structures of both surfaces of the M slab, front and rear, are almost identical. They differ only in some details related by symmetry operations.

The M slab cut from the 5/3-approximant consists of 930 atoms. For electronic structure calculations such a model is too big and on the other hand its thickness  $4.08 \text{ \AA}$  does not sufficiently represent the structure of the bulk. A more tractable model is a model derived from the 3/2-approximant.

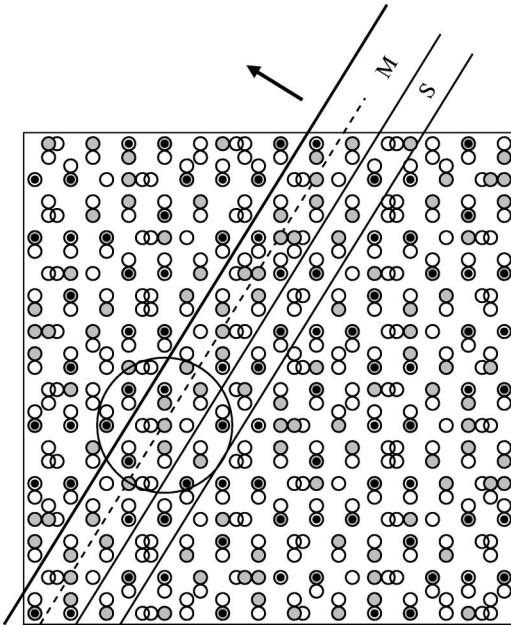


FIG. 3. Side view of the MS and the M models of the  $i$ -AIPdMn surface derived from the  $3/2$ -approximant. The MS model consists of two slabs: an M slab and the adjacent S slab. The M model consists of the M slab only. The dashed line in the middle of the M slab indicates the positions of centers of the  $B$  clusters. The radius of one  $B$  cluster is indicated by the circle. The surface plane dissects the  $B$  clusters. On the other hand the MS model includes the complete bottom part of the  $B$  clusters. The small circles represent projected positions of the atoms, cf. Fig. 1.

We shall consider two variants of the model. The first one consists of two slabs—the M slab and the adjacent S slab. The thickness of this model is  $6.6 \text{ \AA}$  and we find it to be sufficiently large to support the surface. The model includes 535 atoms. We shall consider also a second model consisting of the M slab only that includes 357 atoms. We designate these models as MS and M, respectively. In Fig. 3 the construction of the models is presented. The dashed line in the middle of the M slab indicates the positions of the centers of  $B$  clusters. The radius of one  $B$  cluster is indicated by a circle. It is seen that the MS model representing the bulk termination dissects the  $B$  cluster. While the complete  $B$  cluster consists of 33 atoms, in the truncated cluster six atoms are missing. On the other hand the thickness of the model of  $6.6 \text{ \AA}$  is just sufficient to include the complete lower part of the  $B$  clusters. From the figure it is possible to see that the surface of the M slab is Al-rich. It is also remarkable that in the M slab the Mn atoms are located just at the surface. The structural parameters of the considered models are listed in Table I.

### III. COMPUTATIONAL METHODS

The progress of computational methods and the increasing computational power of the available computers allows us to obtain interesting physical information from *ab initio* calculations on highly realistic structural models. The charge density distribution and other electronic properties have been

calculated using advanced local-density-functional techniques. We have used the Vienna *ab initio* simulation package VASP<sup>28,29</sup> to perform *ab initio* electronic structure calculations and structural optimizations. The theoretical background of VASP is density-functional theory within the local-density approximation. The wave functions are expanded in plane waves. The Hamiltonian is based on pseudopotentials derived in framework of the projector-augmented-wave (PAW) method.<sup>29</sup> VASP performs an iterative diagonalization of the Kohn-Sham Hamiltonian. The plane-wave basis allows one to calculate Hellmann-Feynman forces acting on the atoms. The total energy may be optimized with respect to the positions of the atoms within the cell. The calculations were performed within the generalized-gradient approximation (GGA).<sup>30</sup> VASP has also been used to calculate charge distributions. The projector-augmented-wave version<sup>29</sup> of VASP calculates the exact all-electron potentials eigenstates and charge densities, hence it produces very realistic valence-electron distributions.

The possibility to calculate the interatomic forces allows us not only to relax the idealized geometrical positions of atoms from the 6D projection and to obtain thus a more realistic model of bulk, but also to investigate possible surface relaxations or reconstructions. We are able to study the change of the positions of atoms at and near the surface relative to the bulk termination in response to the broken bonds at the surface.

The computational cell has an orthorhombic shape. It includes a layer of atoms with a thickness of  $6.6 \text{ \AA}$  (in the case of the MS model) and a  $6 \text{ \AA}$  thick vacuum layer. Although the slabs forming the MS model cut from the cubic approximants have a monoclinic geometry, it is easy to adapt them to an orthorhombic computational cell. The fivefold axis is parallel to the  $c$  axis. The length of the  $b$  edge is equal to the lattice parameter of the cubic approximant,  $b = d_n$ , where  $n$  is the order of the approximant, the length of the cell along the  $a$  axis is given by  $a = b \times \sqrt{(\tau+2)}/\tau$ .

### IV. ATOMIC STRUCTURE AND CHARGE DENSITY DISTRIBUTION AT THE SURFACE

Figure 4(a) shows the atomic structure of the surface of the  $3/2$ -M model derived from the KGB model of bulk  $i$ -AIPdMn. The surface is covered by a periodic approximant of the quasiperiodic P1 tiling.<sup>5</sup> The edge of the P1 tiling is  $7.76 \text{ \AA}$ . The tiling in the figure consists of three different tiles—a regular pentagon, a pentagonal star, and a thin golden rhombus. A general quasiperiodic P1 tiling consists of four species of tiles, in addition to the three listed above a boat can occur. In the  $2/1$ -approximant we observed also a thick golden rhombus, see Table II and Fig. 6 (to be discussed in detail below). The appearance of this motif (which does not appear in the quasiperiodic P1 tiling) is a consequence of the phason strain leading to the formation of a periodic pattern. The two edge-sharing thin rhombi also represent a violation of the matching rules belonging to this phason defect. The P1 tiling is a planar tiling which can be obtained by a projection from a hyperspace. The occupation domain of the P1 tiling is a decagon. The cut-and-projection constructions

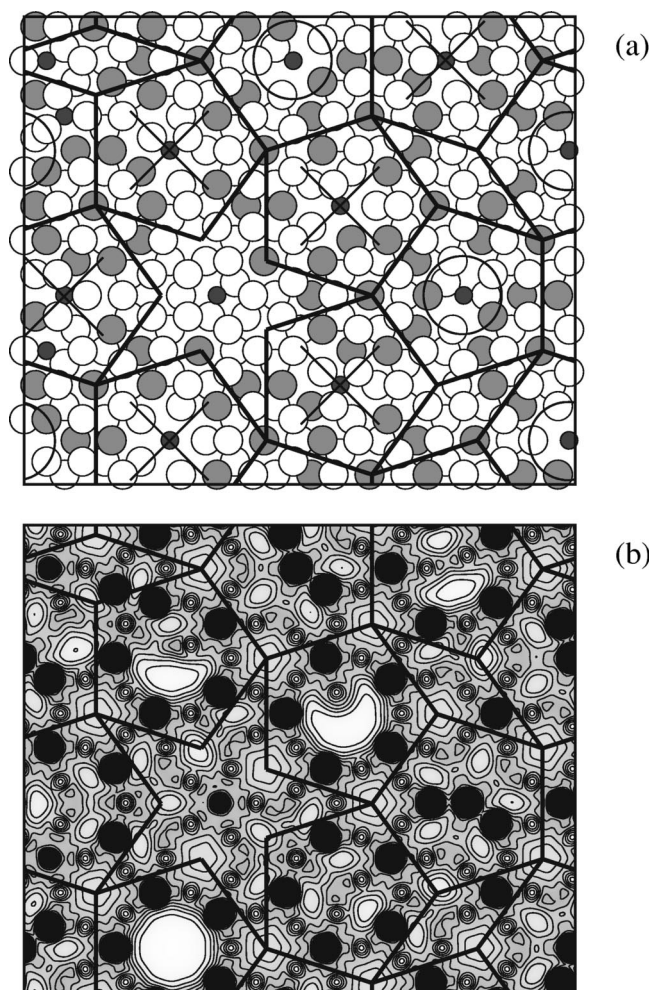


FIG. 4. The atomic structure of the R surface of the M model as represented by the 3/2-approximant. (a) The surface is covered by a part of a P1 tiling. The tiling consists of three tiles: a regular pentagon (P), a pentagonal star (S), and a thin golden rhombus (R). The pentagons may be classified as top ( $P_t$ ) and bottom ( $P_b$ ), as marked by circles and crosses, respectively, cf. text. The quasiperiodic P1 tiling contains in addition a fourth tile, a boat (B) which does not appear in the 3/2-approximant but may be seen in the 2/1-approximant (see Fig. 6). The positions of atoms are displayed by circles: Al: open circles, Pd: shaded circles, and Mn: small closed circles. The bottom part (b) shows the electronic charge density distribution of the same model. The contour plot presents the valence charge density distribution in a plane intersecting the top atomic layer, cf. text. The most striking features are the charge depletions inside some of the pentagonal tiles. They correspond to surface vacancies. The figure demonstrates that most of vertices of the P1 tiling coincide with the positions of Pd atoms in the centers of the truncated  $B$  clusters. Exceptions are the vertices separated by a small distance across a rhombus or a branch of a star. The pentagonal tiles are located at the positions of the  $M$  clusters centered by the Mn atoms. The vertices of the P1 tiling are at charge density minima surrounded by a complete or incomplete pentagon of Al atoms. These charge density minima form pentagonal holes well observed in the high-resolution STM images of the AlPdMn surface, see Ref. 5.

TABLE II. Number of tiles in the approximants to the quasiperiodic P1 tiling.  $P_t$ ,  $P_b$ : pentagons with orientations designated as top, bottom, respectively, B: boat, S: star, and  $R_s$ ,  $R_f$ : skinny and fat rhombuses, respectively.

Model	$N(P_t)$	$N(P_b)$	$N(B)$	$N(S)$	$N(R_s)$	$N(R_f)$
2/1	2	1	1	0	0	1
3/2	4	6	0	1	1	0
5/3	13	12	4	1	5	0

of the KGB model for the structure of bulk  $i$ -AlPdMn and that of the P1 tiling of a fivefold surface are of course closely interrelated. The occupation domain of the planar tiling is a cross section through the 3D domains creating the icosahedral structure. As the surface termination has been chosen at the most densely occupied plane of the quasicrystal, the acceptance domain of the tiling is the maximal cross section of the domain producing the quasiperiodic lattice. For the tricontahedral domain this is just a decagon. Figure 4(a) demonstrates that most of the vertices of the P1 tiling coincide with the positions of the Pd atoms in the centers of the truncated  $B$  clusters. On the other hand the pentagonal tiles are located at the positions of the  $M$  clusters centered by the Mn atoms. Interesting information about the atomic structure of the surface can be derived from the picture of the electronic charge density distribution. Figure 4(b) represents the charge density distribution in the plane of the top atomic layer. The top layer is occupied only by Al and a few ( $\approx 2\%$ ) Mn atoms.<sup>1,6,26</sup> The surface consists of two closely spaced atomic layers separated by a vertical distance of only 0.48 Å. The figure shows that the Pd atoms from the next layer located 0.48 Å below the top layer also contribute to the surface charge density. The Mn atom in the center of the pentagonal star is also located in this subsurface layer. The surface is thus composed of the atoms from the two topmost layers. The chemical composition of the surface of the models is given in Table III. The total surface atomic density of the model derived from the 3/2-approximant is  $n_s = 0.132$  atoms/Å<sup>2</sup>. For two other models derived from the 5/3 and 2/1-approximants the total surface atomic density is  $n_s = 0.134$  atoms/Å<sup>2</sup>. These values are in very good agreement with the experimental value of 0.136 atoms/Å<sup>2</sup> reported by Gierer *et al.*<sup>1</sup>

Figure 4(b) shows charge density minima at the vertices of the P1 tiling occupied by Pd atoms, surrounded by a complete or incomplete pentagon of Al atoms. These charge density minima form the pentagonal holes observed in the high-resolution STM images of the AlPdMn surface.<sup>4,5</sup> The Pd atoms in the centers of the truncated  $B$  clusters are at positions deeper in the slab and their electrons do not contribute to the surface charge density. However, the most striking features of the surface charge density distribution are large charge density minima inside some of the pentagonal tiles. These charge depletions correspond to surface vacancies. These vacancies are the consequence of the irregular structure of the first atomic shell of the  $M$  clusters. In a regular Mackay cluster the first atomic shell consists of 12 atoms forming a small icosahedron. In the  $M$  cluster in  $i$ -AlPdMn

TABLE III. Number of atoms  $N_s$ , partial numbers of atoms at the surface of the approximants, and surface atomic density (in atoms/Å<sup>2</sup>).

Model	$N_s$	$N_s(\text{Al})$	$N_s(\text{Pd})$	$N_s(\text{Mn})$	$n_s$
2/1					
1st layer	41	39	0	2	
2nd layer	24	9	15	0	
together	65	48	15	2	0.134
3/2					
1st layer	105	101	0	4	
2nd layer	66	23	40	3	
together	171	124	40	7	0.132
5/3					
1st layer	283	263	0	20	
2nd layer	161	74	87	0	
together	444	337	87	20	0.134

the central Mn atom has a lower coordination of 7 to 8 atoms,<sup>25</sup> as confirmed by EXAFS experiment.<sup>31</sup> These atoms are distributed on the sites of a small dodecahedron, but their spatial arrangement breaks the local icosahedral symmetry. The vacancies exist in the model of idealized coordinates. The existence of vacancies in the structure of *i*-AlPdMn has been confirmed experimentally by Sato *et al.*<sup>32</sup> The change in the atomic arrangement around the vacancies under structural relaxation is studied in Sec. V. The surface vacancies and their behavior under thermodynamic treatment have been studied experimentally by Ebert *et al.*<sup>33</sup>

The positions of the pentagonal tiles correspond to the positions of the  $M$  clusters. The centers of the  $M$  clusters are projected onto the centers of the pentagonal tiles. In the P1 tiling the pentagonal tiles adopt two different orientations. The orientation of the pentagonal tiles is related to the vertical position of the  $M$  clusters. According to this vertical position of the centers of  $M$  clusters we designate the pentagonal tiles as top and bottom. In the top pentagon the center of the  $M$  cluster is at the top surface of the  $M$  slab. In the bottom pentagon the center of the  $M$  cluster is at the bottom surface of the  $M$  slab. We note that any two neighboring pentagons that share one edge always have opposite orientations. In Fig. 4 the central Mn atoms in the bottom pentagons are near the bottom of the  $M$  slab and therefore they do not contribute to the surface charge density. This contributes to the formation of the pronounced charge density minima associated with the surface vacancies. On the other hand in the top pentagons the central Mn atoms are in the top atomic layer (together with Al atoms) and are well seen in the surface charge density distribution. Figure 4(b) also shows that not only the internal arrangement of the pentagons is irregular, but also the thin rhombuses have irregular decorations. Although the pentagonal star in the figure exhibits a relatively high regularity, an analysis of other approximants reveals that the decoration of the pentagonal star is in general also quite irregular. It is possible to conclude that the quasiperiodic order at the surface is represented by the P1 tiling, but on the other hand internal decoration of the tiles is rather irregular. The irregularities are also well seen in the high-

resolution STM images of the pentagonal AlPdMn surfaces.<sup>3,5</sup> We emphasize that these irregularities exist in the model with idealized positions of atoms and therefore are not a consequence of the relaxation of the atomic positions or a surface reconstruction (see the following Sec. V) which naturally leads to deviations of the positions of the atoms from their ideal positions and hence introduces another degree of irregularity. The spatial modulation of the ideal quasiperiodic structures resulting from long-range interatomic forces has been discussed in detail in our earlier works on higher-order approximants of *i*-AlZnMg and *i*-AlCuLi.<sup>34,35</sup>

## V. RELAXATION OF ATOMIC POSITIONS AND SURFACE RECONSTRUCTION

In general, surfaces of solids can adopt a different structure than the bulk. The existence of unsaturated bonds at the surface can lead to a rearrangement of the positions of the atoms at the surface with a periodicity larger than that of the bulk-terminated surface. Such surface reconstructions are well-known in the case of C, Si, Ge, and many other covalently bonded solids where the recombination of dangling bonds leads to the formation of surface-dimers stabilized by double-bonds and a  $(2 \times 1)$  surface reconstruction.<sup>36,37</sup> Eventually Jahn-Teller distortions cause an asymmetry of the surface dimers and a longer periodicity of the surface reconstruction.<sup>38</sup> In metals, surface reconstruction is observed mainly on the more open surfaces. Prominent examples are the long period reconstructions of the (100) surface of the face-centered cubic  $5d$  metals: a  $(1 \times 5)$  reconstruction has been reported for Ir(100),<sup>39-41</sup> a long-period pseudohexagonal reconstruction for Au(100).<sup>42,43</sup> Here the driving force of the surface reconstruction is the stabilization of the surface by adopting a more close-packed pseudohexagonal arrangement of the atoms. Since the surface termination we have chosen for the fivefold surface of *i*-AlPdMn exposes the most close-packed layer, no similar reconstructions are to be expected. This question was examined experimentally.<sup>3</sup> The fact that the high-resolution STM image can be interpreted by a tiling derived from a model of

the bulk structure<sup>3,5</sup> indicates that in the case of *i*-AlPdMn the surface does not significantly differ from the bulk structure and does not undergo a larger reconstruction. Our methods allow us to approach the problem of surface reconstruction or relaxation more in detail.

One has to distinguish between relaxation of atomic positions in the bulk and the surface reconstruction which is a response to the broken bonds at the surface. We distinguish three variants of our structural model. In model (i) with idealized atomic coordinates the positions of the atoms are obtained directly from the 6D projection. The surface models presented so far were cut out from models of 5/3- and 3/2-approximants with the idealized coordinates of atoms. Models with relaxed coordinates of atoms are more realistic. The position of each atom is shifted to its equilibrium position with respect to the forces acting from the neighboring atoms. There are two possibilities how to perform such relaxation. One possibility is to relax atomic coordinates in the bulk and cut the slab representing the surface from such a bulk-relaxed model [model (ii)]. The other and apparently the most realistic variant of the model is obtained if the relaxation is performed on the slab [model (iii)]. However, the problem with the last variant is that the model must represent a termination of the bulk structure and if the slab is not thick enough, the bulk structure is not stable. A relaxation of the bottom surface of the slab should not have influence on the relaxation of the studied top surface. One frequently used possibility that we have adopted also in our calculations is to fix the positions of the atoms in the bottom part of the slab.

Our computational method is able to calculate interatomic forces. We can therefore relax the model and find the equilibrium position of each atom. Unfortunately, the 3/2-approximant is already too big for such calculations where the electronic structure must be recalculated after each move of the atoms. We have to restrict our relaxation studies to the smaller 2/1-approximant.

In Fig. 5 projections of the positions of the atoms in one unit cell of the 2/1-approximant are displayed. The positions of atoms are projected on the  $(x, y)$  plane along the  $z$  axis. Part (a) of the figure shows the positions in model with idealized coordinates, part (b) presents the result of the structural relaxation. The figure demonstrates the fact known also from other studies<sup>44</sup> that in aluminum-transition-metal quasicrystals the transition metal atoms have low mobility. It is seen that the positions of Mn and Pd atoms change only very little. As expected, the largest displacements are observed for Al atoms from the irregular first shell of  $M$  clusters. The maximal displacement of such an Al atom is 1.71 Å. The average displacement of the atoms is only a small fraction of their diameter. The average displacements of the Mn and Pd atoms are 0.15 and 0.14 Å, respectively. Displacements of the Al atoms are larger, their average value is 0.38 Å.

Figure 6 shows three variants of the model of a fivefold surface derived from an MS slab of the 2/1-approximant. Part (a) shows the surface with idealized positions of atoms [model (i)]. In part (b) the slab representing the surface was cut from a bulk model with relaxed atomic coordinates [model (ii)]. The model (iii) of the surface presented in part (c) is the MS slab with the relaxed surface. The periodic approximant of the P1 tiling superposed on the surface con-

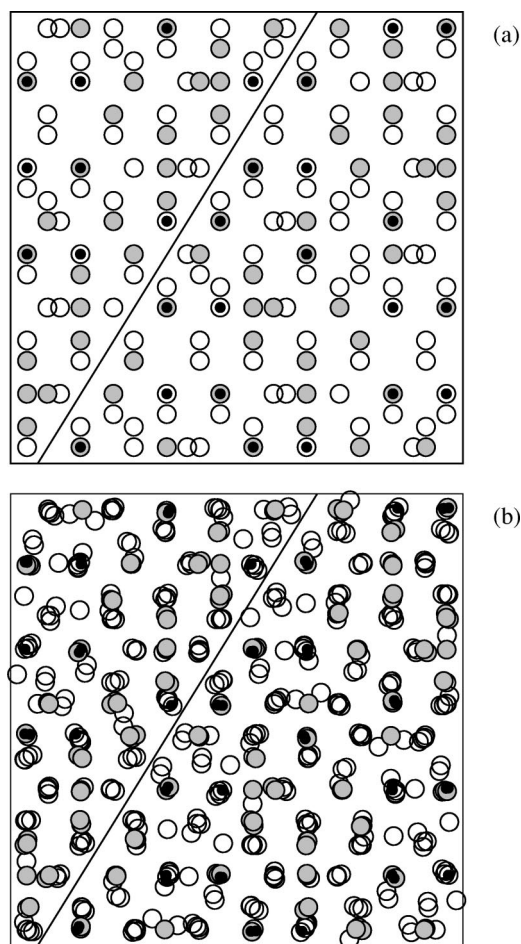


FIG. 5. Projections of the positions of atoms in one unit cell of the 2/1-approximant, Al: open circles, Pd: shaded circles, and Mn: small closed circles. Part (a) of the figure shows the positions in the model with idealized coordinates, part (b) presents the result of the structural relaxation. The figure demonstrates that the positions of Mn and Pd atoms are only little affected by relaxation. The largest displacements are observed for Al atoms from the irregular first shell of  $M$  clusters. The maximal displacement of an Al atom is 1.71 Å. We note that the circles in the figure represent position of the atoms, the actual size of the atoms is  $\approx 4$  times larger. An average atomic displacement is thus only a small fraction of its diameter, cf. text. The straight line shows the position of the cleavage plane.

sists of three pentagons (two top, one bottom), a boat, and one thick and one thin rhombus. A comparison of Figs. 6(a) and 6(b) thus demonstrates the effect of relaxation of the atomic positions in the bulk, Figs. 6(b) and 6(c) give an impression on a degree of the surface relaxation. One observes that the arrangement of atoms belonging to the truncated  $B$  clusters are rather stable. On the other hand a larger reconfiguration of atoms is seen around the centers of the  $M$  clusters. Altogether, since the skeleton of the P1 tiling is preserved and only the atomic decoration is changed, it is more appropriate to speak of surface relaxation than of reconstruction.

A more detailed view on the effect of the surface relaxation is demonstrated in Figs. 7 and 8. In Fig. 7 the charge

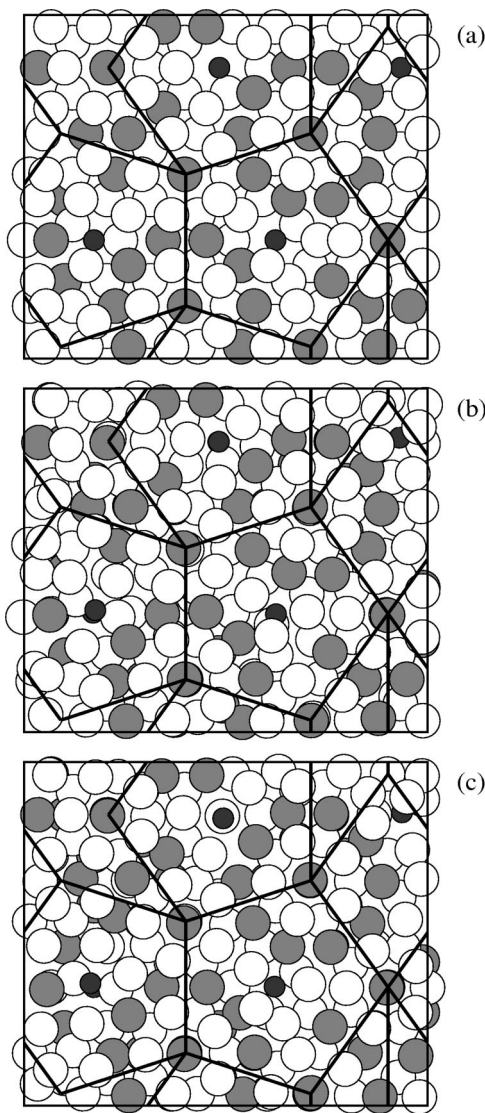


FIG. 6. Three variants of the model of a fivefold (R) surface derived from the 2/1-approximant. Part (a) shows the surface of the MS model with the idealized positions of atoms. In part (b) the MS slab representing the surface was cut from the bulk model with relaxed atomic coordinates. The model of the surface presented in part (c) is the MS slab relaxed after cleavage. The periodic approximant of the P1 tiling consisting of three pentagons, a boat, and a thin and fat rhombus, is superposed on the surface. The positions of atoms are displayed by circles: Al: open circles, Pd: shaded circles, and Mn: small closed circles. A comparison of (a) and (b) thus demonstrates the effect of relaxation of atomic positions in the bulk, the figures (b) and (c) give an impression of the degree of the surface relaxation. One can observe that the arrangement of atoms belonging to the truncated  $B$  clusters is rather stable. On the other hand a larger reconfiguration of atoms is seen around the centers of the  $M$  clusters.

density distribution in the fivefold surface of the 2/1-approximant with idealized coordinates (a) and with a relaxed surface (b) are presented. The contour plots represent cuts of the charge density distribution at the position of the top layer of Al atoms, see line  $ZZ'$  in Fig. 8(a). The  $B$  clusters are marked by dashed circles,  $M$  clusters by dot-dashed

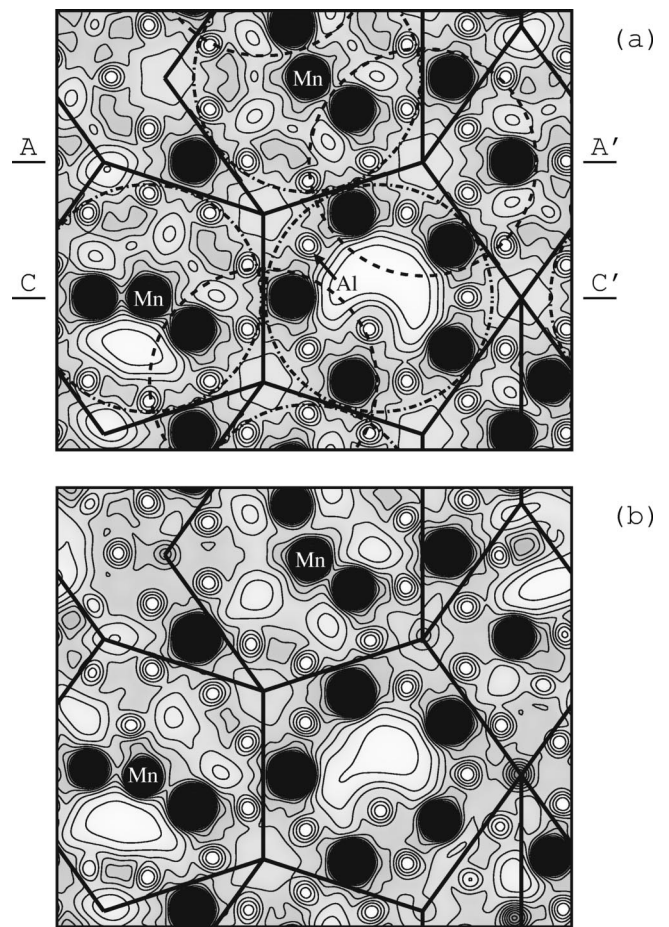


FIG. 7. The valence charge density distribution in the surface of the 2/1-approximant with idealized coordinates (a) and with relaxed surface (b) are presented. The contour plots represent cuts through the charge density distribution at the position of the top layer of the Al atoms, see line  $ZZ'$  in Fig. 8(a). The  $B$  clusters are marked by dashed circles, the  $M$  clusters by dot-dashed circles. The charge density distributions in planes perpendicular to the surface intersecting along lines  $AA'$  and  $CC'$  marked in Fig. 7(a) are presented in Fig. 8. The transition metal atoms in the plane create a high charge density, black circles. The Mn atoms are marked explicitly, the remaining black circles are the Pd atoms. The positions of the Al atoms can be recognized as small circular islands of local density minima; one Al atom near the center of the figure is marked explicitly. One can observe that the positions of the Pd and Mn atoms remain almost intact after the surface relaxation. The charge density distribution is changed predominantly inside the pentagonal tiles, i.e., around the centers of the  $M$  clusters. Inside the  $B$  clusters the changes are only rather modest. Pentagonal clusters of Al atoms around the vertices of the P1 tiling are quite stable. The large charge depressions inside the pentagonal tiles correspond to the surface vacancies. In the relaxed surface (b) these depressions are rearranged (cf. text).

circles. The charge density distributions for intersections perpendicular to the surface along lines  $AA'$  and  $CC'$  marked in Fig. 7(a) are presented in Fig. 8.

We are aware that the thickness of the MS model of 6.6 Å is smaller than the thickness of the slabs used in analogous studies of crystalline surfaces. The total thickness of the slab

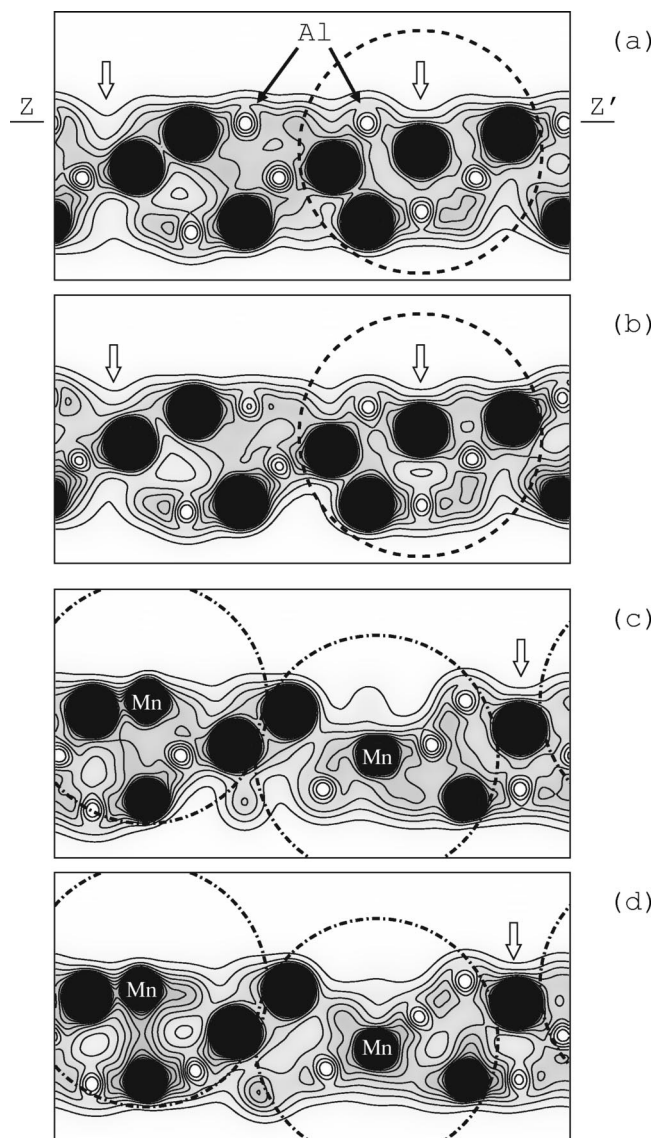


FIG. 8. Sections perpendicular to the surface displaying the valence charge density distribution with idealized coordinates of atoms (a,c) and with relaxed positions (b,d). The contour plots represent cuts of charge density distribution at the position of lines AA' (a,b) and CC' (c,d), i.e., through the centers of the *B* and *M* clusters, respectively, see Fig. 7(a). The *B* clusters are marked by dashed circles, *M* clusters by dot-dashed circles. The charge density distributions for intersections along AA' and CC' are presented. Transition metal atoms contribute by a high charge density, black circles. The Mn atoms are marked explicitly, the remaining black circles are the Pd atoms. The positions of the Al atoms can be recognized as small circular islands of local density minima; two Al atoms in the top atomic layer are marked explicitly. Vertical arrows mark surface charge density minima at the positions of the vertices of the P1 tiling. These charge density minima are well seen in the STM images as dark pentagonal holes.

should be large enough to represent bulk. Our results for the surface charge density in the relaxed models can be affected by the insufficient thickness of our MS model. We attempted to estimate the effect of the slab thickness on the surface charge density distribution by considering two variants of the

TABLE IV. Ideal and relaxed interlayer spacing in the 2/1-MS model (in Å). The second column presents the spacing of atomic layers in the model with ideal positions of atoms. The third column presents the spacing of atomic layers after a relaxation where positions of atoms in the *M* slab are relaxed while in the *S* slab they are fixed. The fourth column presents the spacing after relaxation of position of atoms in both *M* and *S* slabs.

Layers	Ideal	Relaxed <i>M</i> , Fixed <i>S</i>	Relaxed <i>M</i> and <i>S</i>
$d_{12}$	0.481	0.533	0.541
$d_{23}$	0.779	0.789	0.574
$d_{34}$	0.779	0.547	0.912
$d_{45}$	0.481	0.701	0.538
$d_{56}$	1.558	1.556	1.839
$d_{67}$	0.481	0.481	0.154
$d_{78}$	0.481	0.481	0.279

model. In the first variant, during the relaxation the coordinates of atoms in the *S* slab at the bottom of our model were fixed, and only atoms in the *M* slab were allowed to move; in the second variant the positions of all atoms in both *M* and *S* slabs were allowed to relax. Although certain minimal quantitative differences in the surface charge density distribution between both variants of the MS model can be recognized, the substantial physical features of the relaxed models which we report below are the same for both variants.

One observes that the positions of Pd and Mn atoms remain almost unchanged. The charge density distribution is modified predominantly inside the pentagonal tiles, i.e., around the centers of the *M* clusters. Again one can see that inside the *B* clusters the changes are minimal. The pentagonal cluster of Al atoms around the vertices of the P1 tiling are quite stable as well.

Similarly as in the case of the 3/2-approximants shown in Fig. 4(b), the most striking features in the charge distribution are the large charge depressions corresponding to surface vacancies. One such vacancy is located near the center of the figure in the central part of a pentagonal tile above a Mn atom. In the relaxed model this depression becomes shallower. As is well seen in the perpendicular section presented in Figs. 8(c) and 8(d), the charge depression becomes partially filled and shallower after relaxation.

Another surface vacancy is seen in the pentagonal tile near the left side of the figure. Although in the presented sections of the charge density the vacancy seems to be somewhat smaller than the one discussed previously, a closer inspection shows that in fact it is substantially deeper. It can even accept an additional Al atom.

We can conclude that while the TM atoms retain relatively fixed positions at the surface and thus propagate the quasiperiodic order of the bulk, the Al atoms are more mobile, particularly around the center of the *M* clusters and thus contribute more to the surface relaxation. The largest degree of relaxation is observed at the positions of the surface vacancies originating from the low coordination of the center of *M* clusters. The important result is that the structure of the P1 tiling is conserved if the atoms in the surface are free to move.

Figures 8(a)–8(d) provide an impression of the surface corrugation. Vertical arrows mark surface charge density minima at the positions of the vertices of the P1 tiling. These charge density minima are well seen in the high-resolution STM images where they manifest themselves as dark pentagonal holes. They usually occur in the centers of the perfect pentagonal Al clusters that exist inside the *B* clusters. However, they are observed also in the centers of incomplete pentagonal clusters, see Fig. 8. On the other side the bright protrusions seen in the high-resolution STM images apparently correspond to the positions of the TM atoms at the surface.

Zheng *et al.*<sup>6</sup> analyzed the structural relaxation of the quasicrystalline *i*-AlPdMn surface using x-ray photoelectron diffraction. They found differences in the interlayer spacing of near-surface layers compared with the spacing of atomic layers in the bulk. They considered several termination planes and in average the distance between the top two layers is reduced from the ideal value  $d_{12}=0.48$  Å by  $-0.06$  Å, and the spacing between the second and fourth layer increased from the ideal value of  $d_{24}=1.56$  Å by  $0.04$  Å. The results of a similar study for our 2/1-MS model are listed in Table IV.

We relaxed the surface by minimizing the forces acting on the atoms in the M slab, while in the S slab the atoms were fixed at their bulk positions. Contrary to the conclusions from the XPD analysis in our model the surface relaxation leads to an increase of the interlayer spacing between the two topmost layers. In our study  $d_{12}$  increased from its ideal value by  $0.05$  Å to  $0.53$  Å. This discrepancy need not be in contradiction with the experimental data, as the reported experimental value is an average over several different terminations. The scatter of the experimental values is considerable. For two out of nine considered terminations the interlayer spacing  $d_{12}$  increased by  $0.046$  and  $0.067$  Å, i.e., in a reasonable agreement with our value. To demonstrate that the interlayer spacing sensitively depends on the choice of the termination plane we looked at the changes of the interlayer spacing in both free surfaces of the MS slab, top and bottom. When coordinates of atoms in both M and S slabs of the MS model were relaxed the interlayer spacing of the two top layers remained essentially the same,  $d_{12}$  increased from its ideal value of  $0.48$  Å by  $0.06$  Å to  $0.54$  Å, but the interlayer spacing of the two bottom layers is substantially reduced,  $d_{78}$  decreased from its ideal value of  $0.48$  Å by  $0.20$  Å to  $0.28$  Å. If one takes an average of these two values the result is a contraction of the interlayer spacing at the surface by  $0.13$  Å.

## VI. ELECTRONIC STRUCTURE

Our structural models of the surface consist of hundreds of atoms. Calculations of the electronic structure by VASP for such big models, particularly when performing the structural relaxation, are extremely difficult. Therefore we had to restrict the calculations of the electronic structure to the  $\Gamma$ -point only. The electronic density of states can be calculated also by the tight-binding LMTO method<sup>45</sup> in the atomic-sphere approximation (ASA) which is considered to be less accurate, but with this method a denser sampling of

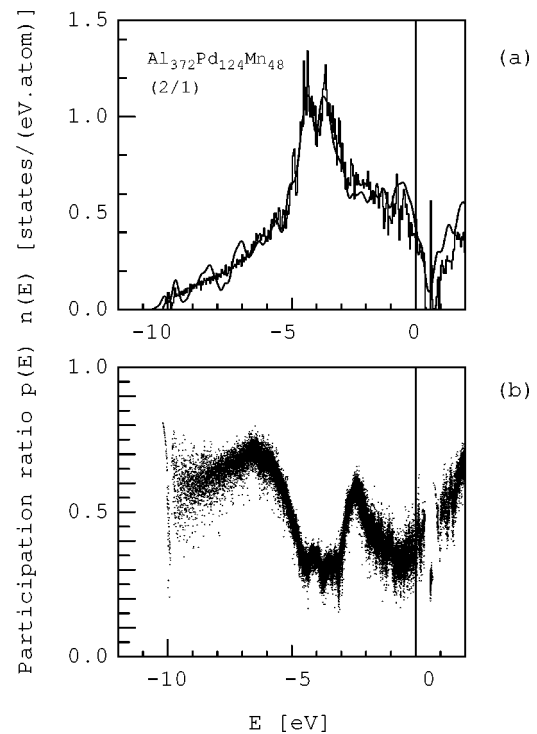


FIG. 9. Part (a) compares the density of states of the 2/1-approximant calculated by VASP ( $\Gamma$ -point only, full line) and TB-LMTO (fine  $\mathbf{k}$ -point mesh, histogram). The *i*-AlPdMn quasicrystal belongs to the structural class of quasicrystals exhibiting semiconducting behavior at the correct band filling (electron-per-atom ratio) (Ref. 46). In the TB-LMTO result one observes above the Fermi level a real gap in the DOS with localized states in the middle of the gap. In the VASP result the gap appears only as a deep pseudogap. Part (b) shows the participation ratio of the eigenstates, high values around 0.6 correspond to propagating states, low values around 0.3 correspond to states with a moderate degree of localization.

the reciprocal space is possible. Figure 9(a) compares the density of states of the 2/1-approximant calculated by both methods, VASP (using a Gaussian smearing of the  $\Gamma$ -point eigenvalues) and TB-LMTO (using a histogram with a bin-width of  $0.035$  eV). The histogram represents the DOS calculated by TB-LMTO from the eigenvalues at 24  $\mathbf{k}$ -points in the irreducible Brillouin zone. The *i*-AlPdMn quasicrystal belongs to the structural class of quasicrystals that can exhibit semiconducting behavior if perfectly ordered (both structurally and chemically) and at the proper band filling (i.e., the correct electron per atom ratio).<sup>46</sup> In the histogram resulting from TB-LMTO calculations achieving a high resolution in  $\mathbf{k}$ -space one observes a real gap in the DOS  $0.4$  eV above the Fermi level with a group of localized states in the middle of the gap. In the VASP results the gap manifests itself only as a deep pseudogap. Figure 9(b) shows the participation ratio of the eigenstates. For the definition of the participation ratio see, e.g., Refs. 46 and 47. The participation ratio can be considered as a measure of localization: high values around  $p \approx 0.6$  correspond to propagating states, low values close to  $p \sim 1/N$  correspond to localized states. Values around  $p \approx 0.3$  correspond to states with a moderate degree

of localization. One can clearly recognize delocalized Al  $s,p$  states in the energy region from the bottom of the band at  $-10.5$  eV to  $\approx -6$  eV. The double-peak in the DOS extending from  $-4.5$  to  $-2.5$  eV corresponds to the Pd  $d$  band. The low participation ratio in this region is in agreement with a more localized character of the  $d$  states. The states around the Fermi level states are formed predominantly by Mn  $d$  states and again the participation ratio indicates their higher degree of localization. In Fig. 9(b) one can also clearly see the gap with a group of localized states in the center. We assume that a genuine semiconducting quasicrystal can be achieved by a modest degree of chemical substitution on the TM sites. Although the existence of the band gap in the electronic spectrum of the approximant to  $i$ -AlPdMn is a highly interesting phenomenon (it indicates a possible insulatinglike behavior) this question is not the subject of this work. For more details on a possible semiconductivity of the quasicrystals we refer the reader to our recent works on this topic.<sup>46</sup>

Figure 9(a) demonstrates that the VASP results with the  $\Gamma$ -point only agree quite well with the TB-LMTO results in the energy region where states are localized and hence have lower dispersions. On the other hand in the region of delocalized Al  $s,p$  states these states have large dispersions and the agreement of VASP results with those of TB-LMTO is not so satisfactory. Nevertheless, our interest is focused to the region around the Fermi level where the  $\Gamma$ -point approximation used at the VASP calculations is reasonable.

Figure 10 shows the total and partial DOS of the MS and M models derived from the 2/1 approximant. For comparison we present also the data for the bulk. In the electronic structure of the MS model the deep pseudogap just above the Fermi level has disappeared, at the surface the DOS at Fermi level is higher than in the bulk. This is a significant observation as Fournée *et al.*<sup>7</sup> came to a similar conclusion from their analysis of photoelectron and Auger electron spectroscopies. The partial DOS show that both Mn and Al states contribute to this enhancement. The Pd band exhibits only very small changes in the region around the Fermi level. On the other hand, one observes a significant shift of the whole Pd band to lower binding energies. In comparison with the position of the Pd  $d$  band in the bulk the Pd  $d$  band at the surface is shifted by  $\approx 0.5$  eV towards the Fermi level. Similarly, the Mn  $d$  band is shifted towards the Fermi level, completely covering the pseudogap.

The M slab consists of five atomic layers only. The centers of the Bergman clusters are located in the central layer. This layer has a low atomic density. In the M slab of the 2/1 approximant there are only 4 Pd atoms in this layer. The remaining four atomic layers are surface layers. The DOS of the M slab is thus formed predominantly by contributions from the surface atoms. The dashed lines in Fig. 10 represent the total and partial DOS of the M slab. One observes a significant change of the Mn partial DOS. The Mn  $d$  band is substantially narrowed. The DOS at the Fermi level is greatly enhanced. This enhancement is the consequence of the fact that all Mn atoms of the model are located just at the surface. This suggests that the enhancement of DOS at the Fermi level observed in the photoemission studies of the surface could have its origin in the presence of the Mn atoms at the surface.

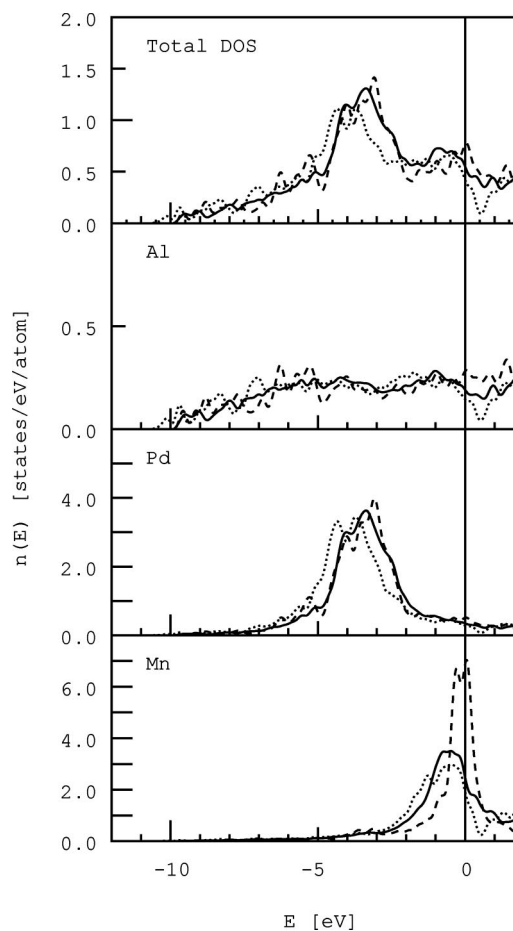


FIG. 10. Total and partial DOS of the MS (full lines) and M (dashed lines) slabs based on the 2/1-approximant. For the comparison the data for the bulk (dotted lines) are also presented. In the electronic DOS of the slabs representing the surface the deep pseudogap just above the Fermi level has disappeared, the DOS at the Fermi level is increased for both the MS and M models. In comparison with the position of the Pd  $d$  band in bulk the Pd  $d$  band in the surface model is shifted towards the Fermi level. Note a significant enhancement of the Mn partial DOS of the M model.

## VII. DISCUSSION AND CONCLUSIONS

Our work represents an *ab initio* investigation of the stability, structure, and electronic properties of a quasicrystalline surface. Density-functional investigations of a crystalline surface already have a long tradition—for recent reviews see, e.g., Duke and Plummer,<sup>48</sup> Groß,<sup>49</sup> and references therein. Most investigations have concentrated on the low-index surfaces describable by small surface cells [a  $p(1 \times 1)$  for the surfaces of elemental metals], allowing to treat even thick slab models with modest computational effort. Relatively few studies have been devoted to the more demanding task of modeling vicinal surfaces [see Spišák<sup>50</sup> for an *ab initio* study of Cu(11 $n$ ) surfaces with  $n$  up to 11] or to the surfaces of 5 $d$  metals showing long-period reconstructions.<sup>51</sup> The investigation of a quasicrystalline surface demands an even greater computational effort. Therefore the present paper reports an *ab initio* study of a quasicrystalline surface.

Like in our work on the electronic structure of bulk quasicrystals<sup>25,52</sup> we follow a strategy of approaching the quasicrystalline limit by investigating a series of rational approximants to the quasicrystalline structure. For *i*-AlPdMn our approximants are based on cut and projection models with triacontahedral acceptance domains according to the Katz-Gratis-Boudard model. A fivefold surface is prepared by cleaving the bulk structure along a plane perpendicular to a fivefold axis such that a layer with a high atomic density is exposed at the surface. A first important result is that the atomic arrangement in this surface can be described in terms of a P1-tiling,<sup>5</sup> the decagonal acceptance domains of the tiling corresponding to the maximal cross sections of the triacontahedra defining the three-dimensional structure of the bulk. Most of the vertices of the P1 tiling are occupied by Pd atoms (except those vertices separated by a short distance across a rhombus or the arm of a pentagonal star); the decoration of the tiles is determined by cuts through the Bergman and pseudo-Mackay clusters defining the icosahedral structure of the bulk.

An analysis of the surface electron density has been performed for idealized structure models based on the 3/2 approximant with up to 357 atoms per computational cell. The charge-density analysis shows local minima at the vertices of the P1 tiling which are observed in the STM pictures as dark spots<sup>3,4</sup> and deep minima in the center of some of the pentagonal tiles created by surface vacancies. Again, the existence of these surface vacancies is in agreement with experimental observations.<sup>33</sup>

The central question, however, is whether the idealized structural model for the surface is sufficiently stable to serve as a useful model for a real surface. Structural optimizations have been performed for two slab models of different thickness derived from the 2/1 approximant. The larger of these models contains 205 atoms per cell. The results of careful structural optimizations demonstrate that the skeleton of the P1 tiling fixed by the positions of the Pd atoms remains stable. On the other hand, the arrangement of the atoms decorating the tiles undergoes considerable modification at the surface, the Al atoms in particular being subject to quite substantial displacements from their idealized positions. The effect of these relaxations is to flatten the charge-density

minima associated with the surface vacancies. In addition, we calculate quite large relaxations of the interlayer distances. However, these results must admittedly be considered with some caution because the amount of interlayer relaxation shows some dependence on the thickness of the slab representing the surface—here our calculations certainly cannot achieve the degree of convergence usual for crystalline surfaces.

The electronic structure of the quasicrystals of the icosahedral AlPdMn class is characterized by a deep pseudogap just above the Fermi level representative of a considerable degree of covalency in the Al-TM interactions (for a more detailed discussion we refer to our earlier work<sup>46</sup>). The investigation of the surface electronic structure shows that the metallic character is enforced at the surface. The structure-induced minimum in the partial Al-DOS is leveled out as a consequence of the strong relaxations of the near-surface Al atoms. The Pd *d* band undergoes a substantial shift towards lower binding energies. The Mn *d* band is also up-shifted and for the Mn atoms closest to the surface the partial DOS peaks at the Fermi level. Both effects contribute to eliminate the pseudogap. The high Mn-DOS at  $E_F$  might even lead to a magnetic polarization of the surface-Mn atoms, but an investigation of this question will probably request a large slab model.

In summary: Our *ab initio* investigations show that the structure of the fivefold surface of *i*-AlPdMn as described by the P1-tiling is stable. Atomic relaxations affect only the decoration of the tiles and the interlayer distances. The degree of covalence characteristic for these icosahedral alloys is reduced at the surface. The present work is devoted to the investigation of quasiperiodic elemental overlayers, using our model of the fivefold surface as a template.

#### ACKNOWLEDGMENTS

This work has been supported by the Austrian Ministry for Education, Science and Art through the Center for Computational Materials Science. M. K. also thanks the Grant Agency for Science of Slovakia (No. 2/5096/25) and the Agency for Support of Science and Technology (Grants No. APVT-51021102, APVT-51052702, SO-51/03R80603) for support.

<sup>1</sup>M. Gierer, M. A. Van Hove, A. I. Goldman, Z. Shen, S.-L. Chang, P. J. Pinhero, C. J. Jenks, J. W. Anderegg, C.-M. Zhang, and P. A. Thiel, *Phys. Rev. B* **57**, 7628 (1998).

<sup>2</sup>R. D. Diehl, J. Ledieu, N. Ferralis, A. W. Szmodis, and R. McGrath, *J. Phys.: Condens. Matter* **15**, R63 (2003).

<sup>3</sup>L. Barbier, D. Le Floch, Y. Calvayrac, and D. Gratias, *Phys. Rev. Lett.* **88**, 085506 (2002).

<sup>4</sup>T. M. Schaub, D. E. Bürgler, H.-J. Güntherodt, and J.-B. Suck, *Phys. Rev. Lett.* **73**, 1255 (1994).

<sup>5</sup>Z. Papadopolos, G. Kasner, J. Ledieu, E. J. Cox, N. V. Richardson, Q. Chen, R. D. Diehl, T. A. Lograsso, A. R. Ross, and R. McGrath, *Phys. Rev. B* **66**, 184207 (2002).

<sup>6</sup>J. C. Zheng, C. H. A. Huan, A. T. S. Wee, M. A. Van Hove, C. S. Fadley, F. J. Shi, E. Rotenberg, S. R. Barman, J. J. Paggel, K. Horn, P. Ebert, and K. Urban, *Phys. Rev. B* **69**, 134107 (2004).

<sup>7</sup>V. Fournée, P. J. Pinhero, J. W. Anderegg, T. A. Lograsso, A. R. Ross, P. C. Canfield, I. R. Fisher, and P. A. Thiel, *Phys. Rev. B* **62**, 14049 (2000).

<sup>8</sup>R. McGrath, J. Ledieu, E. J. Cox, and R. D. Diehl, *J. Phys.: Condens. Matter* **14**, R119 (2002).

<sup>9</sup>M. Cornier-Quiquandon, A. Quivy, S. Lefebvre, E. Elkaim, G. Heger, A. Katz, and D. Gratias, *Phys. Rev. B* **44**, 2071 (1991).

<sup>10</sup>A. Katz and D. Gratias, *J. Non-Cryst. Solids* **153-154**, 187 (1993).

- <sup>11</sup>M. Boudard, M. de Boissieu, C. Janot, G. Heger, C. Beeli, H.-U. Nissen, H. Vincent, R. Ibberson, M. Audier, and J. M. Dubois, *J. Phys.: Condens. Matter* **4**, 10149 (1992).
- <sup>12</sup>M. de Boissieu, P. Stephens, M. Boudard, C. Janot, D. L. Chapman, and M. Audier, *J. Phys.: Condens. Matter* **6**, 10725 (1994).
- <sup>13</sup>D. Gratias, F. Puyraimond, M. Quiquandon, and A. Katz, *Phys. Rev. B* **63**, 024202 (2000).
- <sup>14</sup>V. Elser, *Philos. Mag. B* **73**, 641 (1996).
- <sup>15</sup>Z. Papadopolos, P. Kramer, and W. Liebermeister, in *Proceedings of the International Conference on Aperiodic Crystals*, edited by M. de Boissieu, J.-L. Verger-Gaugry, and R. Currat (World Scientific, Singapore, 1997), pp. 173–181.
- <sup>16</sup>P. Kramer, Z. Papadopolos, and W. Liebermeister, in *Proceedings of the 6th International Conference on Quasicrystals*, edited by S. Takeuchi and T. Fujiwara (World Scientific, Singapore, 1998), pp. 71–76.
- <sup>17</sup>A. Yamamoto, *Acta Crystallogr., Sect. A: Found. Crystallogr.* **A52**, 509 (1996).
- <sup>18</sup>A. Yamamoto, H. Takakura, and A. P. Tsai, *Phys. Rev. B* **68**, 094201 (2003).
- <sup>19</sup>A. Quandt and V. Elser, *Phys. Rev. B* **61**, 9336 (2000).
- <sup>20</sup>G. Kasner, Z. Papadopolos, P. Kramer, and D. E. Bürgler, *Phys. Rev. B* **60**, 3899 (1999).
- <sup>21</sup>E. Cockayne, R. Phillips, X. B. Kan, S. C. Moss, J. L. Robertson, T. Ishimasa, and M. Mori, *J. Non-Cryst. Solids* **153-154**, 140 (1993).
- <sup>22</sup>C. R. Lin, S. T. Lin, C. R. Wang, S. L. Chou, H. E. Horng, J. M. Cheng, Y. D. Yao, and S. C. Lai, *J. Phys.: Condens. Matter* **9**, 1509 (1997).
- <sup>23</sup>J. Delahaye, J. P. Brison, and C. Berger, *Phys. Rev. Lett.* **81**, 4204 (1998).
- <sup>24</sup>G. W. Zhang and Z. M. Stadnik, in *Proceedings of the 5th International Conference on Quasicrystals*, edited by C. Janot and R. Mosseri (World Scientific, Singapore, 1995), pp. 552–555.
- <sup>25</sup>M. Krajčí, M. Windisch, J. Hafner, G. Kresse, and M. Mihalkovič, *Phys. Rev. B* **51**, 17355 (1995).
- <sup>26</sup>Z. Papadopolos, P. Pleasants, G. Kasner, V. Fournée, C. J. Jenks, J. Ledieu, and R. McGrath, *Phys. Rev. B* **69**, 224201 (2004).
- <sup>27</sup>Z. Shen, C. R. Stoldt, C. J. Jenks, T. A. Lograsso, and P. A. Thiel, *Phys. Rev. B* **60**, 14688 (1999).
- <sup>28</sup>G. Kresse and J. Furthmüller, *Comput. Mater. Sci.* **6**, 15 (1996); *Phys. Rev. B* **54**, 11169 (1996).
- <sup>29</sup>G. Kresse and D. Joubert, *Phys. Rev. B* **59**, 1758 (1999).
- <sup>30</sup>J. P. Perdew and Y. Wang, *Phys. Rev. B* **45**, 13244 (1992).
- <sup>31</sup>A. Sadoc and J. M. Dubois, *J. Non-Cryst. Solids* **153-154**, 83 (1993); *Philos. Mag.* **66**, 541 (1992).
- <sup>32</sup>K. Sato, Y. Takahashi, H. Uchiyama, I. Kanazawa, R. Tamura, K. Kimura, F. Komori, R. Suzuki, T. Ohdaira, and S. Takeuchi, *Phys. Rev. B* **59**, 6712 (1999).
- <sup>33</sup>P. Ebert, M. Yurechko, F. Kluge, T. Cai, B. Grushko, P. A. Thiel, and K. Urban, *Phys. Rev. B* **67**, 024208 (2003).
- <sup>34</sup>M. Krajčí and J. Hafner, *Phys. Rev. B* **46**, 10669 (1992).
- <sup>35</sup>M. Windisch, J. Hafner, M. Krajčí, and M. Mihalkovič, *Phys. Rev. B* **49**, 8701 (1994).
- <sup>36</sup>B. B. Pate, *Surf. Sci.* **165**, 83 (1986).
- <sup>37</sup>J. Furthmüller, J. Hafner, and G. Kresse, *Europhys. Lett.* **28**, 659 (1994); *Phys. Rev. B* **53**, 7334 (1996).
- <sup>38</sup>P. Krüger and J. Pollmann, *Phys. Rev. Lett.* **74**, 1155 (1995).
- <sup>39</sup>N. Bickel and K. Heinz, *Surf. Sci.* **163**, 435 (1985).
- <sup>40</sup>K. Johnson, Q. Ge, S. Titmuss, and D. A. King, *J. Chem. Phys.* **112**, 10460 (2000).
- <sup>41</sup>A. Schmidt, W. Meier, L. Hammer, and K. Heinz, *J. Phys.: Condens. Matter* **14**, 12353 (2002).
- <sup>42</sup>P. Heilmann, K. Heinz, and K. Müller, *Surf. Sci.* **83**, 487 (1979).
- <sup>43</sup>V. Fiorentini, M. Methfessel, and M. Scheffler, *Phys. Rev. Lett.* **71**, 1051 (1993).
- <sup>44</sup>F. Gähler and S. Hocker, *J. Non-Cryst. Solids* **334-335**, 308 (2004).
- <sup>45</sup>O. K. Andersen, D. Jepsen, and M. Šob, in *Electronic Band Structure and its Applications*, edited by M. Youssouff (Springer, Berlin, 1987).
- <sup>46</sup>M. Krajčí and J. Hafner, *Phys. Rev. B* **68**, 165202 (2003).
- <sup>47</sup>M. Krajčí, J. Hafner, and M. Mihalkovič, *Phys. Rev. B* **65**, 024205 (2002).
- <sup>48</sup>*Frontiers in Surface and Interface Science*, edited by C. B. Duke and E. W. Plummer (Elsevier, Amsterdam, 2002).
- <sup>49</sup>A. Groß, *Theoretical Surface Science* (Springer, Berlin, 2003).
- <sup>50</sup>D. Spišák, *Surf. Sci.* **489**, 151 (2001).
- <sup>51</sup>D. Spišák and J. Hafner, *Surf. Sci.* **546**, 27 (2003).
- <sup>52</sup>J. Hafner and M. Krajčí, *Phys. Rev. B* **47**, 11795 (1993).